RESEARCH LETTER

Nod-Like Receptor Pyrin-Containing Protein 6 (NLRP6) Is Up-regulated in Ileal Crohn's Disease and Differentially Expressed in Goblet Cells

A contributing factor in the development of ulcerative colitis (UC) and Crohn's disease (CD) is aberrant signaling of the innate immune complex known as the inflammasome. The inflammasome regulates the production of interleukin (IL)1β and drives downstream inflammatory pathways. In this study of human tissue (ethics approval: H11930), we provide evidence for the disease-specific up-regulation of NLRP6 transcript and protein in ileal CD and describe an NLRP6-expressing goblet cell (GC) located predominantly in the upper portion of the intestinal crypt. Patient demographic details are provided in Supplementary Table 1.

By using paired quiescent and active biopsy specimens from UC and CD patients we found that the expression of NLRP6 increased with disease activity. In ileal CD we report a 131-fold ($P < .001$) increase in NLRP6 expression compared with a 3.9-fold ($P = .03$) increase in colonic CD (Figure 1A). The increase in IL1β expression was concomitant with increased messenger RNA levels of other inflammasome-related genes such as NLRP1, NLRP3, NLRC4, NLRP12, and AIM2 (Figure 1B and Supplementary Figure 1A and B), suggesting IL1β
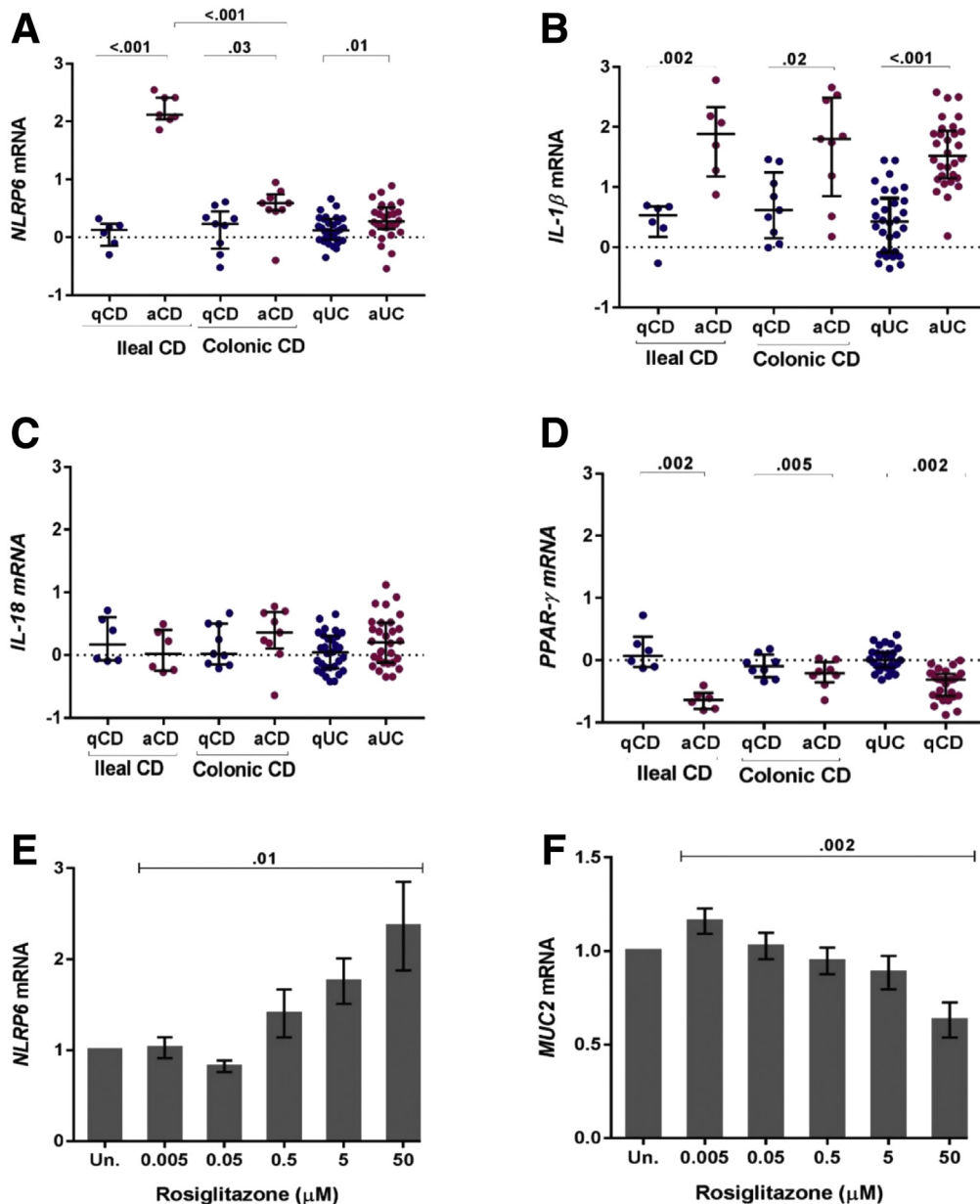

Figure 1. The effect of disease activity and rosiglitazone treatment on the expression of NLRP6-related genes. (A–D) Paired colon biopsy specimens from quiescent (q) and active disease (a) in ileal CD (n = 6), colonic CD (n = 9), and UC patients (n = 30). Relative gene expression of individual biopsy specimens expressed as log$_{10}$-fold change. *Horizontal lines* indicate the median relative expression and *error bars* represent the interquartile ranges. (E and F) Gene expression of NLRP6 and MUC2 in LS174T cells treated with rosiglitazone (5–50,000 nmol/L). Levels are relative to ethanol-treated control cells. Data are expressed as means ± SEM of 3 independent experiments performed in duplicate. The significance threshold was $P < .05$. Un, unstimulated.
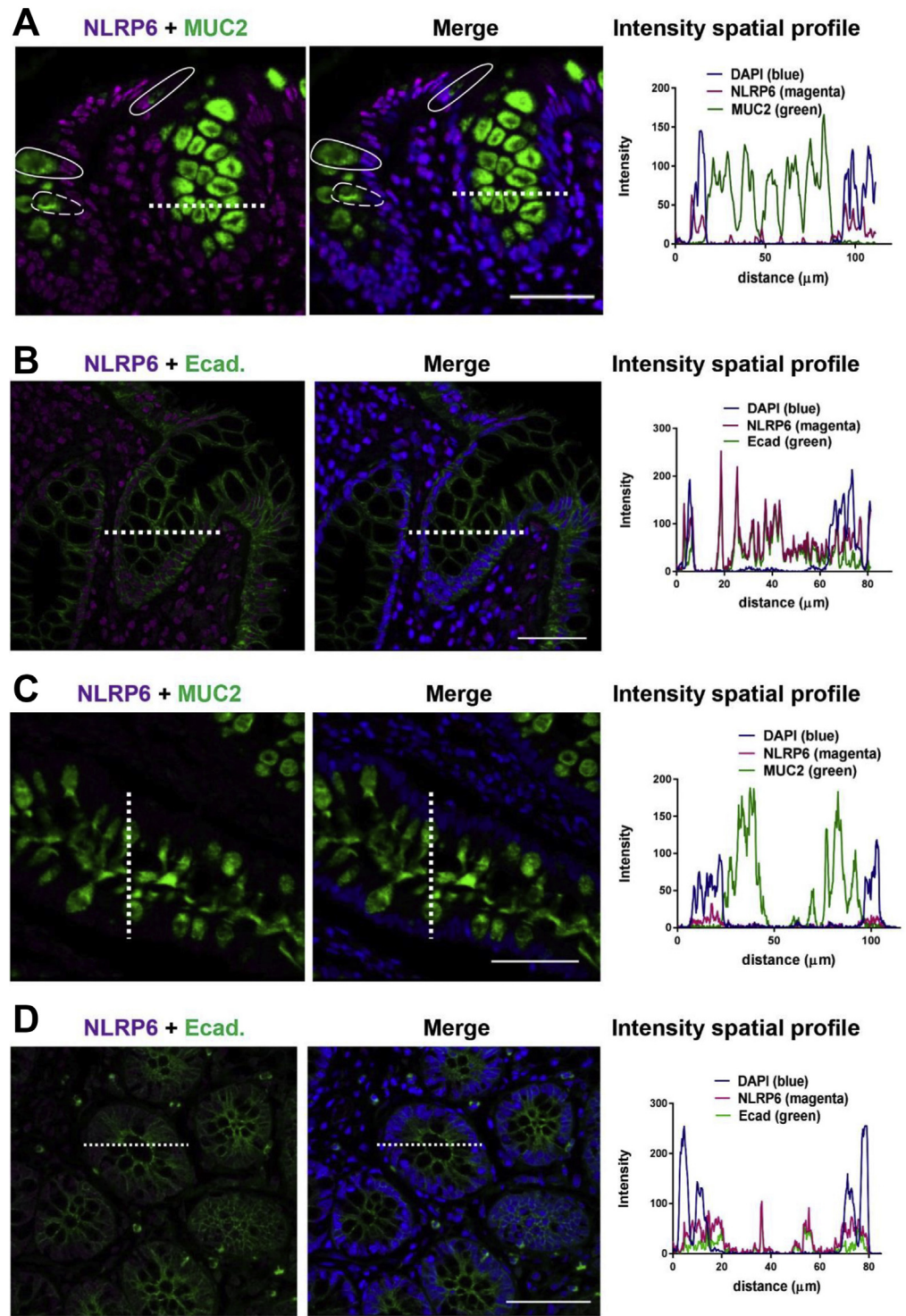
Figure 2. The differential NLRP6 expression in ileal CD goblet cells and overlap of NLRP6/E-cadherin fluorescence signals. Representative immunofluorescence confocal images of NLRP6 (magenta), MUC2 (green), in (A) active ileal CD colon biopsy specimens and (B) normal colon biopsy specimens. *Solid line* indicates goblet cells with high NLRP6 expression. *Dashed line* indicates goblet cell with minimal NLRP6 expression. Representative immunofluorescence confocal images of NLRP6 (magenta) and E-cadherin (green) in (B) active ileal CD biopsy specimens and (D) normal colon biopsy specimens. Spatial profiling is indicated by the *straight dotted line*. Nuclei were stained with 4',6-diamidino-2-phenylindole (DAPI, *blue*), original magnification for all images: 400×. *Scale bars*: 50 μm. Ecad, E-cadherin.

maturation by inflammasome activation is not solely NLRP6-dependent.

Interestingly, the expression of *IL18* remained constant despite variations in *NLRP6* expression (Figure 1*C*). Mouse models have indicated discrepancies regarding the association of NLRP6 with the production of IL18. For example, Nlrp6 deficiency has been associated with low levels of IL18[1] and the induction of intestinal IL18 has been shown to be NLRP6-dependent.[2] However, Normand et al[3] reported no NLRP6-dependent changes in the transcript abundance of IL18 in tumoral and nontumoral biopsy specimens procured from Nlrp6+/+ and Nlrp6-/-

mice. In agreement with Normand et al,[3] this study reports no change in the expression of *IL18* despite localized *NLRP6* expression in inflamed human CD or UC biopsy tissue, suggesting *IL18* expression is not *NLRP6*-dependent.

NLRP6 was found to be highly expressed in colon biopsy specimens from active ileal CD patients and localized to the epithelial cell layer, myofibroblasts, neutrophils, and monocytic lineage cells of the lamina propria (Supplementary Figure 2). Previously, NLRP6 expression in the normal human gut has been described as restricted to the duodenum, jejunum/ileum, and absent from the colon.[4] In contrast, murine Nlrp6 is highly expressed in the small and large intestine.[3]

In mice, Nlrp6 has been shown to regulate goblet cell mucin production and secretion,[5,6] and direct self-renewal and proliferation of epithelial cells.[3] By using immunofluorescence confocal microscopy we sort to ascertain the spatial relationship of NLRP6 to the major mucin protein MUC2 and the epithelial cell marker E-cadherin. The fluorescence signal of NLRP6 was not present in the MUC2 granules (Figure 2A and C), but overlapped the fluorescence signal of E-cadherin (Figure 2B and D). Both myofibroblasts and E-cadherin contribute to epithelial cell structure and renewal. Colonic myofibroblasts are a major source of modulators of the Wnt signaling pathway, which governs approximately 80 genes involved in the differentiation, proliferation, and upward migration of gastrointestinal epithelial cells. Cellular adhesion, maturation, and the correct placement of Paneth and goblet cells is dependent on the proper expression of E-cadherin.[7] Given the high expression of NLRP6 in colonic myofibroblasts and the tight association with E-cadherin, one can speculate that NLRP6 may play a role in epithelial cell positioning and migration.

In active ileal CD biopsy specimens, prominent NLRP6 expression was observed in a number of upper crypt GCs whereas other GCs remained NLRP6 negative (Figure 2A). In the murine system, Birchenough et al[6] identified a sentinel goblet cell localized to the crypt opening that undergoes expulsion and compound exocytosis in an NLRP6-dependent manner. The expelled sentinel goblet cell triggered an intercellular signal via gap junctions that increased cytoplasmic Ca^{2+} and induced Muc2 secretion in adjacent responsive goblet cells. Interestingly, we found the production of MUC2 to be increased in active ileal CD and reduced in active UC (Supplementary Figures 2 and 3).

Transcriptional regulation of *NLRP6* by peroxisome proliferator-activated receptor-γ (*PPAR*-γ) has been proposed based on the presence of binding sites for PPAR-γ and retinoid X receptor upstream of the promotor region of NLRP6.[8,9] We found the expression of *PPAR*-γ to be reduced in active UC and CD (Figure 1D), and that exposure of LS174T colonic epithelial cells to the PPAR-γ agonist rosiglitazone induced *NLRP6* but repressed *MUC2* expression (Figure 1E and F). Previously, the expression of *PPAR*-γ has been reported as reduced in active UC and comparable with normal colon in active CD.[10] Taken altogether, our results suggest that *MUC2* expression is independent of *NLRP6* activity, however, there is insufficient evidence to suggest the negative regulation of *NLRP6* by *PPAR*-γ.

This study has been instrumental in highlighting inconsistencies in NLRP6 expression, IL18 processing, and *MUC2* expression between murine models of chemically induced colitis and human inflammatory bowel disease. NLRP6 now can be regarded as an additional diagnostic tool for distinguishing ileal CD from colonic CD and terminal ileum involved UC. Future work needs to address if there is a therapeutic benefit in switching on NLRP6 in active UC or if disabling NLRP6 improves disease activity in ileal CD.

NICOLE RANSON,[1] MARK VELDHUIS,[2,3]
BRENT MITCHELL,[2,3]
SCOTT FANNING,[2,3] ANTHONY L. COOK,[4]
DALE KUNDE,[1] RAJARAMAN ERI,[1]
[1]School of Health Sciences
[4]Wicking Dementia Research and Education Centre, Faculty of Health, University of Tasmania, Launceston, Tasmania, Australia

[2]Launceston General Hospital, Launceston, Tasmania, Australia
[3]St Vincent's Hospital, Calvary Health Care, Launceston, Tasmania, Australia
Corresponding author: e-mail: rderi@utas.edu.au.

References

1. Elinav E, et al. Cell 2011; 145:745–757.
2. Levy M, et al. Cell 2015; 163:1428–1443.
3. Normand S, et al. Proc Natl Acad Sci U S A 2011;108:9601–9606.
4. Gremel G, et al. J Gastroenterol 2015;50:46–57.
5. Wlodarska M, et al. Cell 2014; 156:1045–1059.
6. Birchenough GM, et al. Science 2016;352:1535–1542.
7. Schneider MR, et al. PLoS One 2010;5:e14325.
8. Levy M, et al. Trends Immunol 2017;38:248–260.
9. Kempster SL, et al. Am J Physiol Gastrointest Liver Physiol 2011; 300:G253–G263.
10. Dou X, et al. Oncol Lett 2015; 10:1259–1266.

Abbreviations used in this letter: **CD, Crohn's disease; GC, goblet cell; IL, interleukin; PPAR, peroxisome proliferator-activated receptor; UC, ulcerative colitis.**

Most current article

Supplementary Materials and Methods

Ethics

The study was conducted by the University of Tasmania, in collaboration with local gastroenterologists, St Vincent's Private Hospital, and Launceston General Hospital. Human ethics was approved by the University of Tasmania (ethics approval: H11930). All participant in this study provided informed written consent or parental consent and were between ages 15 and 80 years. All authors had access to the study data and reviewed and approved the final manuscript.

Study Participants and Biopsy Collection

A total of 85 patients presenting for routine colonoscopy investigations between June 2012 and June 2014 were recruited for this study. Inflammatory bowel disease patients were excluded if they were experiencing co-existing irritable bowel syndrome or non–inflammatory bowel disease–associated gastrointestinal bleeding at the time of colonoscopy. Inflammatory bowel disease patients had paired colonic biopsy specimens taken from both inflamed mucosa and noninflamed mucosa. Control patients were excluded if they had a previous history of inflammatory bowel disease or irritable bowel syndrome.

Of the 85 participants, 30 UC patients and 15 CD patients had colonic biopsy specimens taken from both inflamed mucosa and noninflamed mucosa. Ten UC patients and 4 CD patients were in remission at the time of colonoscopy and only had biopsy specimens taken from noninflamed mucosa. Four UC and 2 CD patients presented with colonic disease in its entirety and had biopsy specimens taken from only inflamed mucosa. Twenty control patients had biopsy specimens collected from healthy noninflamed mucosa.

Disease assessment and biopsy location was at the discretion of the treating gastroenterologist (M.V., B.M., and S.F.). Selection for immunohistochemistry or immunofluorescence microscopy analysis was based on patient pathology reports and only biopsy specimens from the descending left colon with active disease features were chosen.

Cell Culture

The human colorectal adenocarcinoma cell line, LS174T, was obtained from Sigma-Aldrich, Corp (St. Louis, MO), and cultured in RPMI Medium 1640 (Gibco, Gaithersburg, MD) supplemented with 10% fetal bovine serum (Life Technologies, Carlsbad, CA), GlutaMAX (Life Technologies), and 1% penicillin/streptomycin (Cellgro, Corning Life Sciences, Tewksbury, MA). Cells were maintained in a $37^\circ C$ incubator with 5% CO_2 and a relative humidity of 95%. Cells between passages 6–10 were seeded at $1.2 \times 10^5/cm^2$ 1 day before a 6-hour incubation with varying concentrations of rosiglitazone[1] (chemical abstract service number: 122320-73-4; Sigma-Aldrich Corp). Experiments were performed in duplicate on 3 separate occasions.

Gene Expression Analysis

Total RNA was extracted from tissue biopsy specimens and LS174T cells using the RNeasy Plus Mini Kit (Qiagen, Venlo, The Netherlands). RNA quality and concentration were determined using the Experion automated electrophoresis system (Bio-Rad, Hercules, CA). RNA was reverse-transcribed to complementary DNA using the iScript complementary DNA synthesis kit (Bio-Rad). Quantitative real-time polymerase chain reaction was performed on a StepOne analyzer (Applied Biosystems, CA) using a TaqMan Universal PCR Master mix (Applied Biosystems, Foster City, CA) and on-demand gene-specific primers for human NLRP6, IL1β, and IL18. Gene expression was quantified using the comparative (delta-delta CT) method in which the threshold cycle was normalized to the reference gene, eukaryotic translation elongation factor (EEF2).

Transcriptional Profiling Using RNA Sequencing

Total RNA was extracted from quiescent and active disease colon biopsy specimens using the RNeasy Plus Mini Kit (Qiagen). RNA quality and concentration were determined using the Agilent 2100 Bioanalyzer system (Agilent, Santa Clara, CA). Library preparation was performed using the SureSelect targeted RNA capture kit (Integrated Sciences, Sydney, Australia). Libraries were validated on an Illumina HiSeq 2000 Sequencer (v2 100-bp pair-end reads) (Illumina, San Diego, CA) at a concentration of 80 Mb. Base-calling was performed offline using Galaxy (https://galaxyproject.org).

Immunohistochemistry Analysis

Immunohistochemistry was performed on 10% (vol/vol) formalin-fixed, paraffin-embedded, left colon biopsy specimens. Sections were deparaffinized and subjected to 0.01 mol/L citrate buffer (pH 6.0) antigen retrieval at $121^\circ C$ for 4 minutes in a decloaking chamber. Endogenous peroxidases were quenched by a 5-minute incubation in 10% H_2O_2 in methanol. Nonspecific binding was blocked by a 20-minute incubation in Biocare background Sniper solution (BS966G; Biocare, Concord, CA). Immunostaining was performed using specific antibodies against NLRP6 (NBP2-31372; Novus Biologicals, Littleton, CA) and MUC2 (H:300 sc-15334; Santa Cruz Biotechnologies, Dallas, TX) at room temperature for 1 hour. Samples were incubated with a horseradish peroxidase polymer (MRH53BL10; Biocare) for 30 minutes, stained with Betazoid 3,3′-diaminobenzidine tetra hydrochloride chromogen (BDB900B; Biocare), counterstained with hematoxylin, dehydrated, and mounted with distyrene, plasticizer, and xylene mounting media. Slides were examined using an IX71 microscope (Olympus Australia, Melbourne, Australia).

Confocal Immunofluorescence Microscopy

Immunofluorescence staining was performed on 10% vol/vol formalin-fixed, paraffin-embedded, left colon biopsy specimens. Sections were deparaffinized and subjected to 0.01 mol/L citrate buffer (pH 6.0) antigen retrieval at $121C^\circ$ for 4 minutes in a decloaking chamber. Nonspecific binding was blocked by a 1-hour incubation in blocking buffer (0.1 mol/L phosphate-buffered saline/5% normal

goat serum/0.05% Tween-20) at room temperature in the dark. Immunofluorescence staining was performed using specific antibodies against NLRP6 (NBP2-31372; Novus Biologicals), MUC2 (H:300 sc-15334 and F-2: sc-515032l; Santa Cruz Biotechnologies), and E-cadherin (NCH-38, M3612; Dako North America, CA) in the dark, at room temperature for 1 hour or alternatively overnight at 4°C. Sections then were incubated for 1 hour in the dark with 1 or more Alexa Fluor–conjugated secondary antibodies (Cell Signalling Technology, Danvers, MA). Section were incubated with Hoechst 33342 (62249; ThermoFisher Scientific, Waltham, MA) diluted in phosphate-buffered saline and mounted with ProLong Gold Antifade (P36930; ThermoFisher Scientific). Slides were examined using a FV1200 Laser Scanning Confocal Inverted Microscope (Olympus Australia).

Data Analysis

Analysis of quantitative real-time polymerase chain reaction data from colon biopsy specimens and rosiglitazone-treated LS174T cells was performed using Microsoft Excel and GraphPad Prism software (version 7.0; GraphPad Software, Inc, La Jolla, CA). Colon biopsy gene expression was compared with a healthy control group and normalized to the housekeeping gene EEF2. Group differences were tested using paired t tests of $\log_{10}$-transformed data. Data are presented as median relative expression and interquartile ranges. Differences between group means for LS174T cells was assessed using 1-way analysis of variance and data are presented as means ± SEM.

Analysis of immunohistochemistry data and spatial intensity profiling was performed using the FIJI version (Dec 2009) of ImageJ software (http://imagej.nih.gov/ij/downloads.html, ImageJ, US National Institutes of Health, Bethesda, MD), and GraphPad Prism (version 7; GraphPad Software, Inc). Group differences and statistical significance were evaluated using a 1-way analysis of variance followed by Dunnett's multiple comparison test. Data are presented as means ± SD. In all presented data the significance threshold was set at $P < .05$.

References

1. Kempster SL, et al. Am J Physiol Gastrointest Liver Physiol 2011; 300:G253–G263.
2. Pullan RD, et al. Gut 1994; 35:353–359.
3. Swidsinski A, et al. Gut 2007; 56:343–350.
4. Lennon G, et al. Colorectal Dis 2014;16:O161–O169.
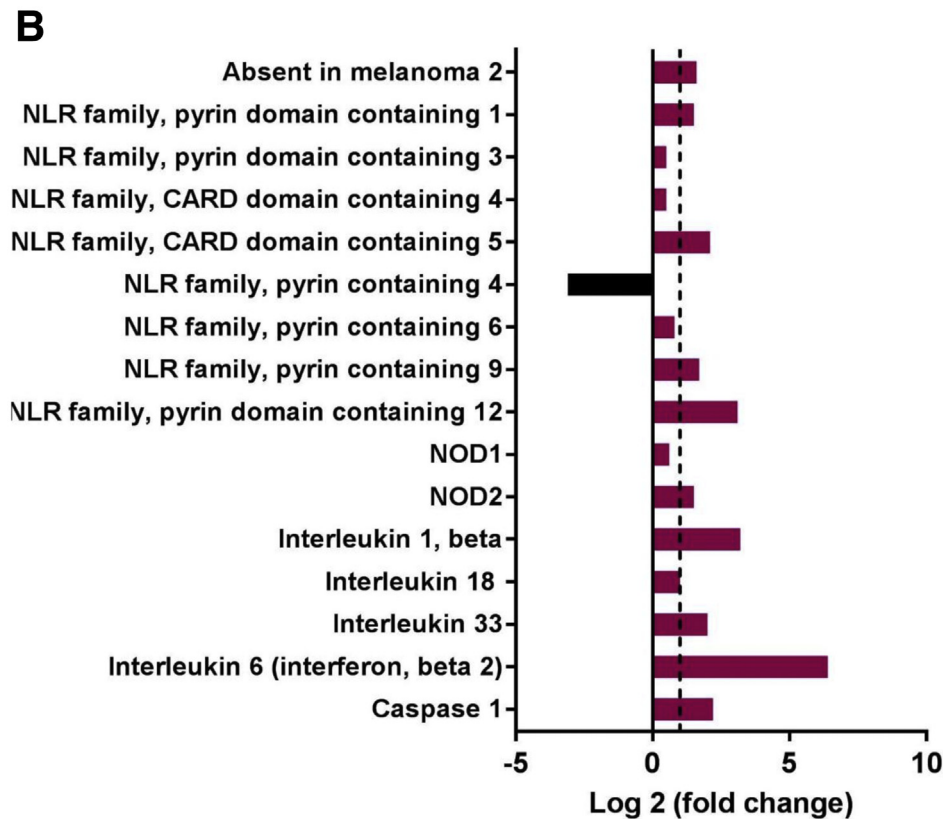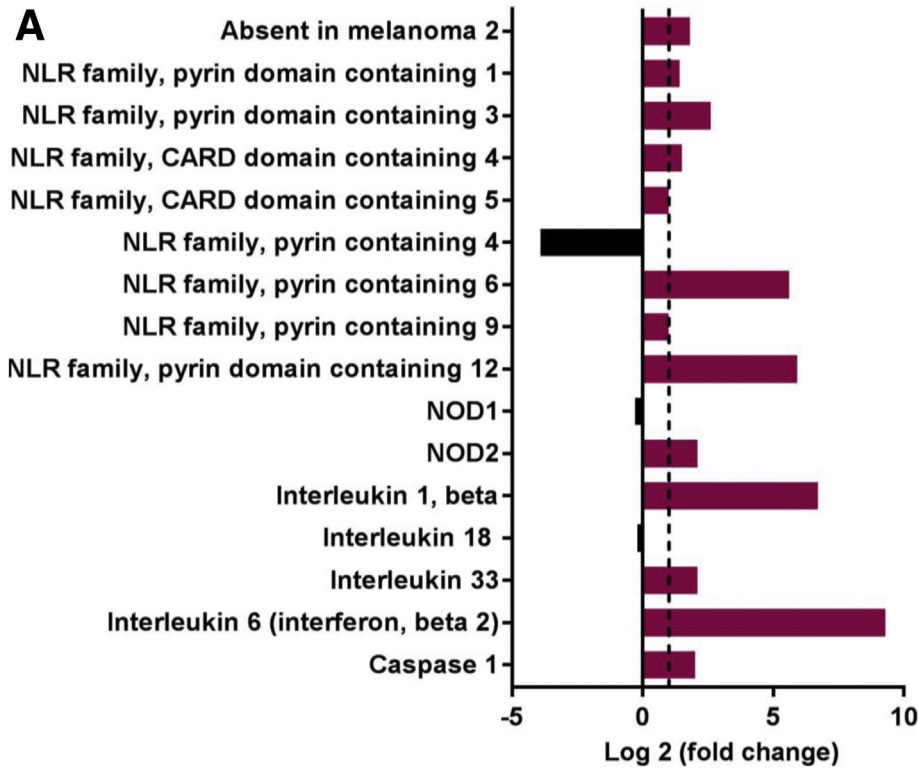5. Birchenough GM, et al. Science 2016;352:1535–1542.

Nod-like receptor pyrin-containing protein 6 (NLRP6) is upregulated in ileal Crohn's disease and differentially expressed in goblet cells
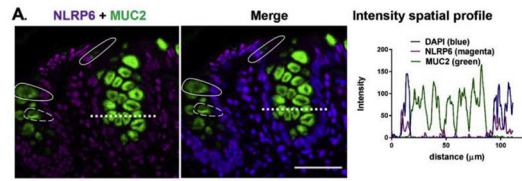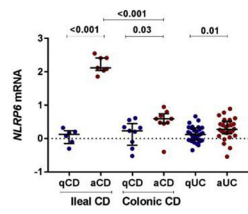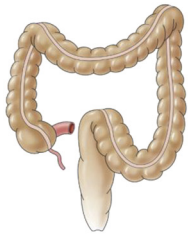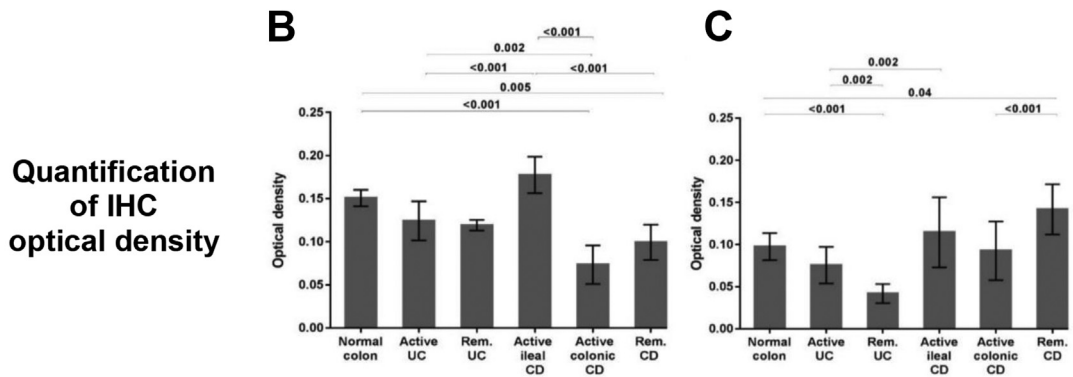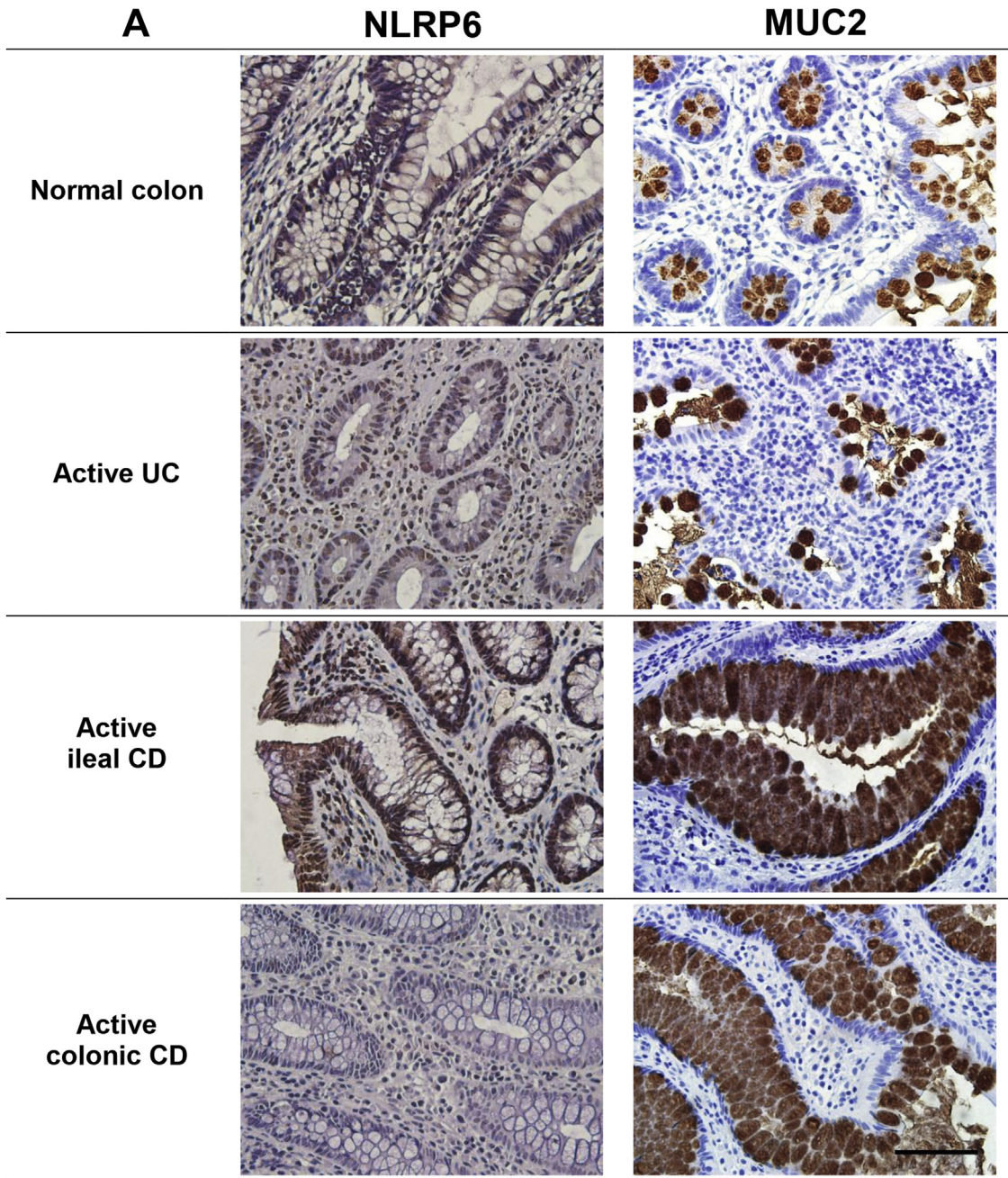

Ileal Crohn's disease

Supplemental Graphical Summary.

A

B

Supplementary Figure 1. Targeted RNA-sequencing analysis of inflammasome-related genes in CD biopsy specimens. (*A*) Targeted RNA-sequencing analysis of ileal CD biopsy specimens (n = 4) during active disease. Gene expression results are expressed as log 2 (fold change), normalized to housekeeping genes and relative to a normal control group (n = 4), which is indicated by the *dotted vertical line*. Up-regulated genes are shown as magenta, down-regulated genes are shown as black. (*B*) Targeted RNA-sequencing analysis of colonic CD biopsy specimens (n = 4) during active disease. Gene expression results are expressed as log 2 (fold change), normalized to housekeeping genes and relative to a normal control group (n = 4), which is indicated by the *dotted vertical line*. Up-regulated genes are shown as magenta, down-regulated genes are shown as black. NOD, nucleotide-binding oligomerization domain containing.

A NLRP6 MUC2

Normal colon

Active UC

Active ileal CD

Active colonic CD

B **C**

Quantification of IHC optical density

Supplementary Figure 2. (*See previous page*). **Representative immunohistochemistry (IHC) images and quantification of NLRP6 and MUC2 expression in left colon biopsies.** All biopsies were paraffin embedded, cut into 3-5 μm sections and incubated with NLRP6 (NBP2-31372, Novus Biologicals, Littleton, CA) and MUC2 (H:300 sc-15334, Santa Cruz Biotechnologies, TX). Images were captured using DP21 microscope camera (Olympus Australia, Melbourne, Australia) attached to an IX71 microscope (Olympus). Images are 400X and scale bar = 50 μm. (*A*) Quantitative (Quant.) analysis of DAB staining in paraffin embedded left colon mucosal biopsies as analysed by IHC. (*B*) NLRP6 expression in sections from normal colon (number of images analysed = 18), active UC (n = 43), remission UC (Rem. UC, n = 20), active ileal CD (n = 34), active colonic CD (n = 18) and remission CD (Rem. CD, n = 12). (*C*) MUC2 expression in sections from normal colon (n = 20), active UC n = 62), remission UC (n = 20), active ileal CD (n = 24), active colonic CD (n = 30), and remission CD (n = 30). The optical intensity of DAB staining was determined using ImageJ software. All data are presented as mean $\pm$ standard deviation. Statistical significance was evaluated using Dunn's multiple comparison One-way ANOVA and the significance threshold was $P < .05$. Here we present contrasting expression patterns for both NLRP6 and MUC2. In active ileal CD, NLRP6 expression is localised to the epithelial cell layer, myofibroblasts, neutrophils and monocytic linage cells residing in the lamina propria. In active UC NLRP6 expression is limited to lamina propria immune cells and absent for the epithelial cell layer. Interestingly, in the normal colon, moderate cytoplasmic NLRP6 expression was present in the epithelial cell layer and scattered within the lamina propria cells. Quantitative analysis of NLRP6 IHC staining confirms the high *NLRP6* expression observed in ileal CD (active ileal CD *vs* active colonic CD, $P < .001$; active ileal CD vs remission CD, $P < .001$). MUC2 expression in active IBD and the normal colon is highly variable in distribution and depth. In active CD, both colonic and ileal the expression of MUC2 is increased while in UC it is reduced. The reduced MUC2 expression in active UC is well established and consistent with previous studies in human derived material.[2-4] Interestingly, there was no change in MUC2 expression in ileal and colonic CD despite the increased NLRP6 in ileal CD. Quantitatively, the expression of MUC2 in active ileal CD was greater than in active UC ($P = .002$).

Normal colon

Active UC

Active ileal CD
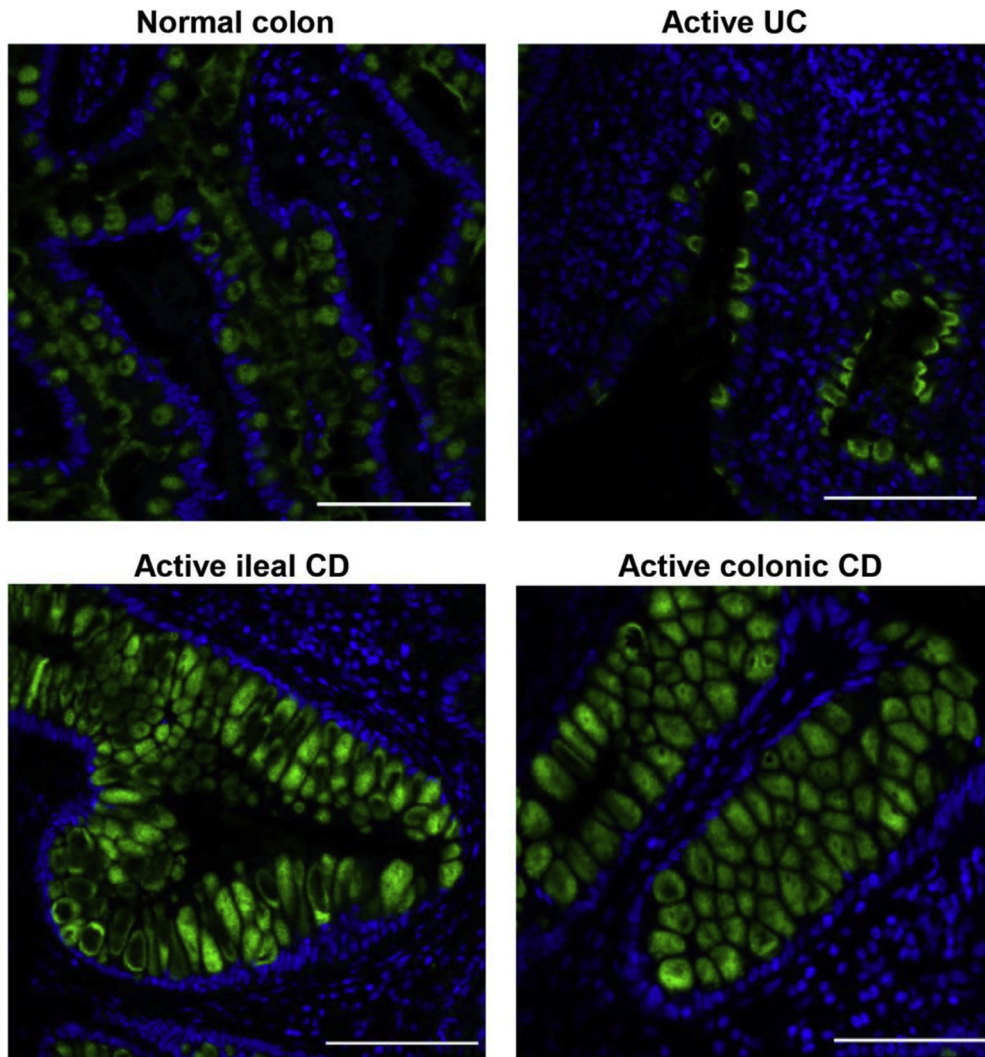
Active colonic CD

Supplementary Figure 3. Representative immunofluorescence images of MUC2 localization in normal colon, active UC, and active ileal and colonic CD. All biopsy specimens were taken from the left colon, paraffin-embedded, cut into 5-μm sections, incubated with MUC2 (H:300: sc15334, 1:200 dilution; Santa Cruz), and visualized using Alexa Fluor 647–conjugated goat anti-rabbit IgG (green). Nuclei were stained with Hoechst 33342 (4′,6-diamidino-2-phenylindole, blue). *Scale bars*: 100 μm for both the 100× and 400× magnification. Here, we present immunofluorescence microscopy images showing the variations in MUC2 architecture. In CD, the MUC2 granules are highly organized and this structural organization is lacking in active UC and in the normal colon. Furthermore, colonic crypts normally contain smaller goblet cell theca containing less MUC2 in the lower crypts and larger MUC2-filled theca in the upper crypt.[5] However, in active ileal CD and active colonic CD we observed large tightly packed theca containing MUC2 granules along the entire crypt length, and the overcrowding of goblet cells often was associated with crypt distortion.

Supplementary Table 1. Demographic Data for Study Participants

Patient category	Patients, n	Age, y	Sex	Disease duration, y
Control patients	20	57 ± 14	11 F, 9 M	-
Paired UC[a]	30	50 ± 18	16 F, 14 M	11 ± 12
Quiescent UC only	10	49 ± 11	6 F, 4 M	15 ± 11
Active UC only	4	39 ± 21	2 F, 2 M	11 ± 13
Paired ileal CD[a]	6	41 ± 16	2 F, 4 M	12 ± 8
Active ileal CD only	1	28	1 M	15
Paired colonic CD[a]	9	46 ± 15	4 F, 5 M	8 ± 4
Active colonic CD only	1	46	1 F	11
Quiescent CD (includes ileal CD and colonic CD) only	4	20 ± 7	3 F, 1 M	9 ± 14

NOTE. All data are shown as means ± SD. The disease duration at the time of biopsy is shown for each group as the mean value ± SD. The average onset of disease can be calculated by subtracting the disease duration from the average age of the patient. Inflammatory bowel disease patients comprised 65 of the total 85 participants, and, of these, 35 were women and 30 were men. The mean age of inflammatory bowel disease patients providing paired biopsy specimens was slightly younger for the CD group (44 ± 16 y) than the UC group (50 ± 18 y). The mean age of the control group was 57 ± 14 years and comprised 11 women and 9 men.

F, females; M, males.

[a]Patients had biopsy specimens taken from quiescent disease and active disease regions.